Hippocampal deletion of $Na_V1.1$ channels in mice causes thermal seizures and cognitive deficit characteristic of Dravet Syndrome

Rachael E. Stein[a,b], Joshua S. Kaplan[a,1], Jin Li[a], and William A. Catterall[a,b,2]

[a]Department of Pharmacology, University of Washington, Seattle, WA 98195; and [b]Neuroscience Program, University of Washington, Seattle, WA 98195

Contributed by William A. Catterall, June 19, 2019 (sent for review April 22, 2019; reviewed by Alan L. Goldin, Holger Lerche, and Philippe Lory)

Dravet Syndrome is a severe childhood epileptic disorder caused by haploinsufficiency of the *SCN1A* gene encoding brain voltage-gated sodium channel $Na_V1.1$. Symptoms include treatment-refractory epilepsy, cognitive impairment, autistic-like behavior, and premature death. The specific loci of $Na_V1.1$ function in the brain that underlie these global deficits remain unknown. Here we specifically deleted *Scn1a* in the hippocampus using the Cre-Lox method in weanling mice. Local gene deletion caused selective reduction of inhibitory neurotransmission measured in dentate granule cells. Mice with local $Na_V1.1$ reduction had thermally evoked seizures and spatial learning deficits, but they did not have abnormalities of locomotor activity or social interaction. Our results show that local gene deletion in the hippocampus can induce two of the most severe dysfunctions of Dravet Syndrome: Epilepsy and cognitive deficit. Considering these results, the hippocampus may be a potential target for future gene therapy for Dravet Syndrome.

epilepsy | *Scn1a* | Dravet | sodium channels | $Na_V1.1$

Dravet Syndrome, also known as Severe Myoclonic Epilepsy of Infancy (SMEI), usually presents before the age of 1 y in children (1, 2). Febrile seizures are the first manifestation of the disease, and they quickly evolve to spontaneous seizures that become intractable and pharmacoresistant (1, 2). Multiple comorbidities accompany the disease, including cognitive and social impairments, hyperactivity, and circadian rhythm and sleep defects (1, 2). The genetic etiology has been largely elucidated, with >80% of patients displaying haploinsufficiency due to a loss-of-function mutation in the *SCN1A* gene encoding the pore-forming α subunit of the brain voltage-gated sodium channel $Na_V1.1$ (3–6).

In mice, *Scn1a* heterozygotes ($Scn1a^{+/-}$) in the C57BL/6 genetic background are an accurate genocopy and phenocopy of the human disease (7–10). They have thermally induced and spontaneous seizures, hyperactivity, cognitive and social impairments, ataxia, circadian rhythm and sleep deficits, and increased risk of sudden unexpected death in epilepsy (SUDEP) (7–17). Although the global mutation is not cell-specific, reduced sodium current has been observed in GABAergic inhibitory neurons in the hippocampus, cerebral cortex, thalamus, and cerebellum, with little or no effect on sodium current in excitatory neurons in C57BL/6 mice (7, 14, 17, 18). Consistent with a major role of inhibitory neurons in this disease, heterozygous deletion of $Na_V1.1$ in forebrain interneurons recapitulates the epilepsy, premature death, cognitive and social deficits, and sleep impairment of Dravet Syndrome (12, 17, 19), and deletions in subsets of interneurons induce specific aspects of these disease phenotypes (10, 20, 21). In contrast, deletion of *Scn1a* in excitatory neurons does not induce disease phenotypes and actually ameliorates the severity of the disease (22).

Although the major symptoms of Dravet Syndrome, including epilepsy, cognitive impairment, and social interaction deficit, are global "whole-brain" phenotypes, it is unknown whether these global phenotypes can be induced by local deletion of the $Na_V1.1$ channel. To address this question, we focused on the hippocampus because the largest deficits in interneuron excitability are observed in the hippocampus in mice with global knockout of $Na_V1.1$ (7, 9, 18). We used viral expression methods to reduce $Na_V1.1$ channels only in the hippocampus, and we determined whether this local gene deletion can induce the global phenotypes of Dravet Syndrome.

Results

Adeno-Associated Virus-Cre Injection Reduces $Na_V1.1$ Expression in Hippocampal Neurons. To selectively reduce $Na_V1.1$ expression in the hippocampus, we utilized the $Scn1a^{lox/lox}$ mouse line, in which exon 25 of the *Scn1a* gene is flanked by two lox-P sites (Fig. 1 *A* and *B*). Previous studies using this $Scn1a^{lox/lox}$ (*Scn1a* Floxed) mouse line demonstrated that introduction of Cre recombinase (Cre) results in excision of exon 25 and subsequent elimination of *Scn1a* mRNA and $Na_V1.1$ protein as tested by PCR and immunocytochemistry with specific antibodies against $Na_V1.1$ (19). Delivery of an adeno-associated virus (AAV) encoding Cre-recombinase into the hippocampus of these mice should result in localized $Na_V1.1$ deletion. We targeted both the dorsal medial and lateral hippocampus of postnatal day 21 mice using a virally expressed active AAV-Cre-GFP construct or an inactive AAV-ΔCre-GFP control (Fig. 1 *A* and *B*). We verified that expression of GFP was present in the hippocampus and largely restricted to that structure (Fig. 1*C*). To assess the activity of Cre, we injected AAV-Cre or AAV-ΔCre into age-matched tdTomato reporter mice (Jax Stock #007914) at P21. We observed reporter signal in the AAV-Cre–injected mice but not in

Significance

Dravet Syndrome is an intractable epileptic disorder that includes cognitive and social-interaction deficits. It is caused by loss-of-function mutations in the brain sodium channel $Na_V1.1$. We asked whether symptoms of Dravet Syndrome could be induced by introducing the mutation only in the hippocampus, a brain region important for learning and memory and for control of brain excitability. Local mutation of $Na_V1.1$ specifically reduced the excitability of inhibitory neurons in the hippocampus. This local mutation caused thermally evoked seizures and spatial learning deficits, which are brain-wide effects. Our results point to a key role for the hippocampus in generating epilepsy and cognitive deficit in Dravet Syndrome and suggest that gene therapy targeting the hippocampus might be effective in this devastating disease.

Author contributions: R.E.S., J.S.K., and W.A.C. designed research; R.E.S., J.S.K., and J.L. performed research; R.E.S. and J.S.K. analyzed data; and R.E.S., J.S.K., and W.A.C. wrote the paper.

Reviewers: A.L.G., University of California, Irvine; H.L., University of Tübingen, Germany; and P.L., Institut de Génomique Fonctionnelle–CNRS, INSERM, University of Montpellier, France.

The authors declare no conflict of interest.

[1]Present address: Department of Psychology, Western Washington University, Bellingham, WA 98225.

[2]To whom correspondence may be addressed. Email: wcatt@uw.edu.

This article contains supporting information online at www.pnas.org/lookup/suppl/doi:10.1073/pnas.1906833116/-/DCSupplemental.

Published online July 25, 2019.

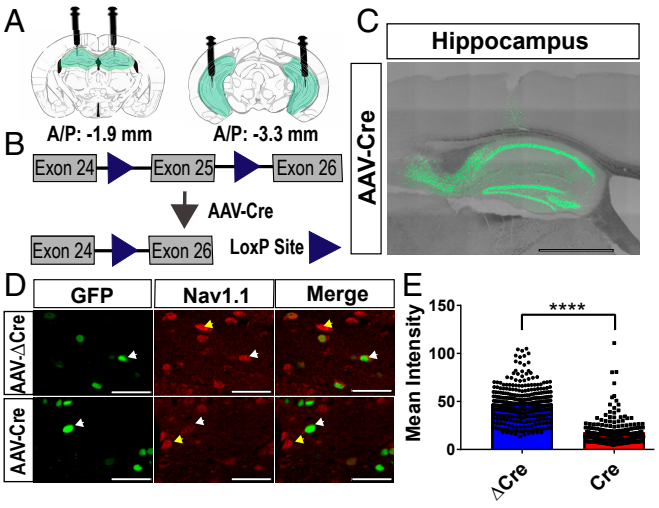

Fig. 1. AAV-Cre injection reduces $Na_V1.1$ expression in hippocampal neurons. AAV-ΔCre and AAV-Cre viruses were injected into the hippocampus of P21 *Scn1a* floxed mice, and tissue was harvested 3 wk later at P42. (*A*) Schematic showing placement of the injection sites (dorsal medial: −1.9 AP, ±1.5 ML, −1.8 DV; ventral lateral: −3.3 AP, ±2.52 ML, −4, −3, −2 DV) in coronal slices of the mouse brain. Green = GFP expression from viral infection. (*B*) Exon 25 of the *Scn1a* gene is excised upon introduction of the AAV-Cre virus. Triangles = loxP sites. (*C*) Representative image of viral infection in a sagittal slice of hippocampus. AAV-Cre = viral infection. (Scale bar, 500 μm.) (*D*) Representative images of $Na_V1.1$ expression in AAV-Cre and AAV-ΔCre infected cells in the hilus of the hippocampus. White arrows indicate $Na_V1.1$-expressing virally infected neurons. Yellow arrows indicate $Na_V1.1$-expressing neurons that are not infected with virus. (Scale bar, 50 μm.) (*E*) Quantification of mean intensity of GFP+ infected hippocampal neurons. Mann–Whitney *U* test: AAV-ΔCre: median = 47.2, n = 305; AAV-Cre: 13.9, n = 208; ****P = < 0.0001.

AAV-ΔCre mice at P42, indicating that AAV-Cre was functional in vivo, whereas AAV-ΔCre was not (*SI Appendix*, Fig. S1). We measured $Na_V1.1$ protein by immunocytochemistry with specific antibodies (19, 23). $Na_V1.1$ antibodies immunostained the cell bodies of neurons in the hippocampus as expected (Fig. 1*D*). Upon quantifying the mean signal intensity of each virally infected cell in AAV-Cre–injected and AAV-ΔCre–injected *Scn1a* floxed mice, we observed a significant reduction of immunocytochemical staining intensity in AAV-Cre–infected neurons vs. controls (AAV-ΔCre: Mean = 47.2 ± 1, n = 305; AAV-Cre: 13.9± 0.9, n = 208; P = <0.0001) (Fig. 1*E*). These results indicate that $Na_V1.1$ protein was reduced on average by 70.6% in AAV-Cre–expressing neurons compared with control AAV-ΔCre–expressing neurons.

***Scn1a* Deletion Reduces Frequency of sIPSCs Recorded in Dentate Granule Cells.** In hippocampal slices, global deletion of $Na_V1.1$ reduces the frequency of spontaneous, action potential-driven IPSCs recorded in excitatory neurons, but does not reduce the frequency of spontaneous EPSCs recorded in the same neurons (12, 24). To test whether AAV-Cre–mediated knockdown of $Na_V1.1$ similarly caused a selective reduction in the excitability of inhibitory interneurons, we compared frequencies of spontaneous action potential-driven inhibitory postsynaptic currents (sIPSCs; E_{Cl} = 0 mV, V_h = −60 mV) and spontaneous excitatory postsynaptic currents (sEPSCs; E_{Cl} = −60 mV, V_h = −60 mV) using whole-cell voltage-clamp techniques in hippocampal dentate granule cells (DGCs) in acutely prepared brain slices at P42 from mice injected with AAV-ΔCre and AAV-Cre at P21. We recorded sIPSCs in the presence of ionotropic glutamate receptor antagonists, 6-cyano-7-nitroquinoxaline-2,3-dione (CNQX; 20 μM) and 2-amino-5-phosphonovaleric acid (APV; 50 μM), to isolate IPSCs from GABAergic interneurons. DGCs from AAV-Cre mice had a strikingly reduced sIPSC frequency (2.15 ± 0.31 Hz, n = 16) compared with DGCs from AAV-Δ-Cre mice (3.79 ± 0.64 Hz, n = 10; t [24] = 2.57, P = 0.02; Fig. 2 *A* and *B*). As a control, we tested whether excitatory neurons similarly showed reduced excitability from AAV-Cre injection by measuring the frequency of sEPSCs in DGCs in the presence of the broad-spectrum $GABA_A$ receptor antagonist, GABAzine (10 μM), to isolate glutamatergic neurotransmission. In the absence of functional GABAergic inhibitory neurotransmission, sEPSC frequency was similar between DGCs from AAV-Cre (0.91 ± 0.16 Hz, n = 8) and AAV-ΔCre mice (0.98 ± 0.12 Hz, n = 11; t [17] = 0.36, P = 0.73; Fig. 2 *B* and *C*). These results support the conclusion that the reduction in sIPSCs is a specific effect of AAV-Cre–mediated knockdown of $Na_V1.1$ in inhibitory neurons rather than a nonspecific effect on all synaptic transmission onto DCGs.

To further test the specificity of the reduction in IPSC frequency caused by AAV-Cre injection, we calculated the effects of GABAzine on the percent change in sEPSCs. If GABAergic inhibitory neurotransmission is specifically reduced in AAV-Cre–expressing mice, the effect of GABAzine on their excitatory neurotransmission should be correspondingly reduced compared with AAV-ΔCre–expressing mice. Consistent with that conclusion, there was a larger GABAzine-induced increase in sEPSC frequency in AAV-ΔCre–expressing mice (85.1 ± 15.9%) than AAV-Cre–expressing mice (24.5 ± 5.79%; t [15] = 3.40, P < 0.01; Fig. 2 *C* and *D*), further indicating that under control conditions, DGCs in AAV-Cre mice have a weaker inhibitory brake on glutamatergic transmission than DGCs in AAV-ΔCre mice.

Reduction of $Na_V1.1$ in the Hippocampus Induces Thermally Evoked Seizures. Febrile seizures are characteristic of early stages of Dravet Syndrome (2). To model febrile seizures in mice, we

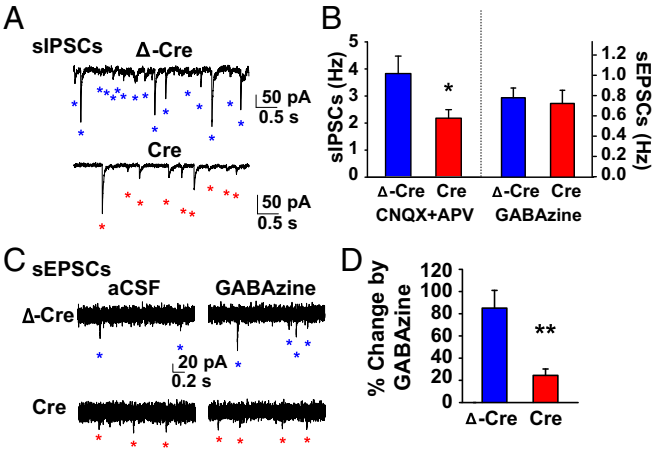

Fig. 2. Selective reduction in $GABA_A$ receptor-mediated transmission in AAV-Cre–injected mice. Voltage-clamp recordings were conducted at P42 on *Scn1a* floxed mice injected at P21 with either AAV ΔCre or AAV Cre (*A*) Representative voltage-clamp recordings (E_{Cl} = 0 mV; V_h = −60 mV) of DGC sIPSCs from -ΔCre (*Top*, blue) and AAV-Cre–injected mice (*Bottom*, red) in the presence of ionotropic glutamate receptor antagonists, CNQX (20 μM) and APV (50 μM). Individual sIPSCs are indicated with an asterisk. (*B*) Summary chart showing the mean sIPSC frequency in CNQX and APV (unpaired two-tailed Student's *t* test: *Left*; AAV-Δ-Cre: 3.79 ± 0.64 Hz, n = 10; AAV-Cre: 2.15 ± 0.31 Hz, n = 17; t [24] = 2.57, P = 0.017) and sEPSC frequency in GABAzine (unpaired two-tailed Student's *t* test: *Right*; AAV-Δ-Cre: 0.98 ± 0.12 Hz, n = 11; Cre: 0.91 ± 0.16 Hz, n = 8; P = 0.73). (*C*) Representative voltage-clamp recordings (E_{Cl} = −60 mV; V_h = −60 mV) of DGC sEPSCs from AAV-Δ-Cre (*Top*, blue) and AAV-Cre–injected mice (*Bottom*, red) in aCSF (*Left*) and the presence of the broad-spectrum $GABA_A$ receptor antagonist, GABAzine (*Right*, 10 μM). Individual sEPSCs are indicated with an asterisk. (*D*) Summary chart showing the percent change in sEPSC frequency caused by GABAzine (unpaired two-tailed Student's *t* test: AAV-ΔCre: 85.1 ± 15.9%, n = 9; AAV-Cre: 24.5 ± 5.79, n = 8; t [15] = 3.40, P = 0.004). Data are represented as mean ± SEM. *P < 0.05; **P < 0.01.

utilized a thermal induction protocol in AAV-Cre–injected and AAV-ΔCre–injected *Scn1a* floxed mice at P42, 3 wk after viral injection (11). After a habituation period, the mice were subjected to a gradual 0.5 °C increase in body temperature every 2 min from 36.5 °C to 41.0 °C, which mimics the increase of body temperature during a fever. During this period, the mice were observed for behavioral epileptic activity, as quantified on the Racine scale of 1 to 5 (25). During this thermal induction paradigm, almost half (44%) of the AAV-Cre–injected mice displayed Racine-4 and -5 seizures at an average temperature of 40.3 ± 0.2 °C, while all AAV-ΔCre–injected mice remained seizure-free (AAV-Cre: $n = 16$; AAV-ΔCre: $n = 17$; $P = 0.0020$) (Fig. 3 *A* and *B*). This average temperature of seizure onset is higher than those observed for global *Scn1a*$^{+/-}$ mice, which have seizures at a mean temperature of 38.5 ± 0.2 °C (11). Visually, we did not observe any spontaneous seizures during handling or behavior, and AAV-Cre–injected mice did not die prematurely, which indicates that they do not have severe spontaneous generalized tonic–clonic seizures that induce SUDEP. These differences are most likely caused by the localized nature of the deletion in the virally injected mice. We assessed and verified viral expression in the hippocampus in each mouse, and we noticed no apparent correlation between areas of viral spread and seizure susceptibility. To verify that these observed behavioral seizures were indeed the result of abnormal electrical activity, we implanted AAV-Cre–injected and AAV-ΔCre–injected mice with electroencephalography (EEG) leads in the left and right cerebral cortex at P35 and subjected these mice to the thermal induction protocol at P42 (Fig. 3*C*). While recordings from AAV-ΔCre mice showed no epileptiform activity (Fig. 3*D*), recordings from AAV-Cre mice displayed interictal spikes, indicative of abnormal electrical activity, during the thermal induction process (Fig. 3*E*). In AAV-Cre–injected animals, thermally induced behavioral seizures were correlated with electrographic seizure activity (Fig. 3*F*). Therefore, local deletion of $Na_V1.1$ in the hippocampus is sufficient to cause interictal epileptiform discharges and thermal induction of seizures, as assessed from measurements of both abnormal behavioral and abnormal electrographic seizure activity.

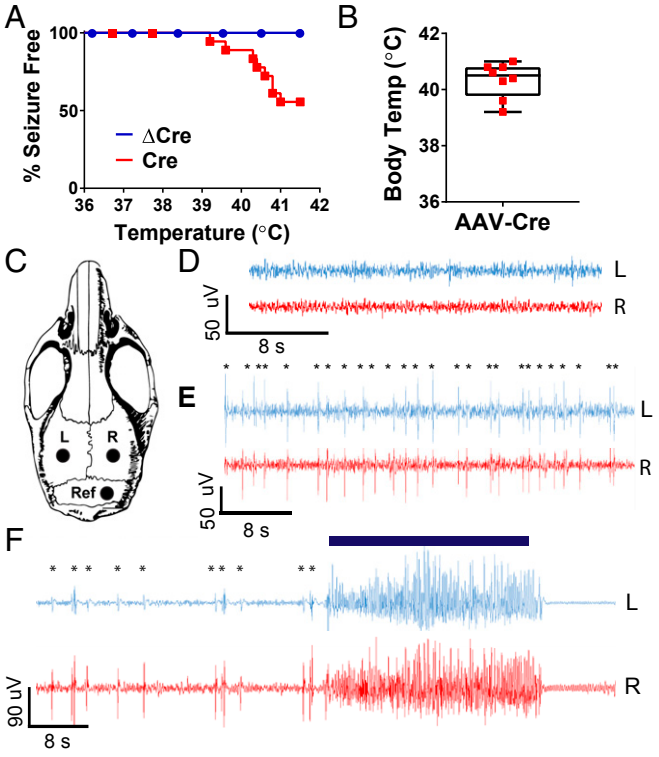

Fig. 3. Reduction of hippocampal $Na_V1.1$ is sufficient to induce thermally evoked seizures. *Scn1a* floxed mice were injected at P21 with AAV-ΔCre or AAV-Cre virus. Mice were either allowed to age to P42 and then thermally induced to test for thermally evoked seizures, or were implanted at P35 with EEG electrodes and then electrographically recorded during thermal induction 1 wk later at P42. (*A*) Percent of AAV-Cre and AAV-ΔCre mice remaining seizure-free after thermal induction. (AAV-ΔCre: 100%; AAV-Cre: 66%). (*B*) Core body temperature at which AAV-Cre–injected mice had seizures (AAV-Cre: 40.3 ± 0.2 °C). (*C*) Schematic of placement of left cortical electrode (L), right cortical electrode (R), and reference electrode (Ref) during EEG implantation surgery. (*D*) Representative cortical EEG trace of an AAV-Cre–injected mouse during the habituation period before the thermal induction protocol. (*E*) AAV-Cre–injected mouse experiencing interictal events during thermal induction protocol; asterisks denote myoclonic events. (*F*) Myoclonic events leading up to a behavioral seizure in an AAV-Cre–injected mouse; asterisks represent myoclonus, blue bar indicates observed behavioral Racine-5 seizure.

Reduction of $Na_V1.1$ in the Hippocampus Causes a Specific Defect in Spatial Learning and Memory. Global *Scn1a* deletion results in several comorbidities, including hyperactivity, social interaction deficit, and cognitive impairment (8, 12, 16). To explore the effects of targeted $Na_V1.1$ reduction in the hippocampus on mouse behavior, we used behavioral assays for locomotion, social interaction, and spatial learning. Locomotor activity was tested in the open field. We found no difference between AAV-Cre–injected mice and AAV-ΔCre–injected mice in total distance traveled, as a measure of hyperactivity, or in the amount of time spent in center of the field, as a measure of anxiety (*SI Appendix*, Fig. S2 *A* and *B*).

To assay the effect of hippocampal *Scn1a* deletion on social behaviors, we subjected the mice to behavioral paradigms that quantify the preference and quality of their interactions with a stranger mouse. In the Three-Chamber Test of social interaction, AAV-Cre and AAV-ΔCre mice similarly demonstrated a significant preference for social interaction by spending more time in close proximity to the cage containing a stranger mouse compared with an identical empty cage, as measured by an interaction ratio ($P < 0.0001$ for both groups) (Fig. 4 *A*–*C*). To examine social interactions in a less confined setting, we used the reciprocal interaction paradigm, which assesses the behavior of mice placed in an open field as they freely interact with a stranger mouse. AAV-Cre mice engaged in a similar number of nose-to-nose interactions, nose-to-anogenital interactions, and rapid escape behaviors as their AAV-ΔCre littermates (Fig. 4*D*). These results indicate that *Scn1a* deletion in the hippocampus is not sufficient to induce impaired social interaction behaviors.

Cognitive abilities are often measured with tests of learning and memory. Novel object recognition memory refers to the ability of a mouse to judge a previously encountered object as familiar vs. a new object as novel. This test is considered a measure of cerebral cortical function when the spatial position of the objects is not part of the test cue (26). Mice with global deletion of *Scn1a* do not display defects in novel object recognition (12). Similarly, both AAV-Cre and AAV-ΔCre mice significantly preferred interacting with a novel object over a familiar object during the novel object recognition paradigm, as measured by an interaction ratio ($P < 0.05$ for both groups) (*SI Appendix*, Fig. S3 *A*–*C*).

As global *Scn1a* deletion results in severe impairments in spatial learning and memory (12, 20), we wondered whether these deficits would also be caused by a local genetic perturbation. We first tested the effects of hippocampal AAV-Cre injection on spatial learning, a task that requires hippocampal function (27–29). To assess spatial learning in the absence of other stimuli, we used the Barnes circular maze (30). Both AAV-Cre and AAV-ΔCre mice were trained three times per day for four consecutive days to find a target hole containing a dark escape box located on the edge of a brightly illuminated circular platform. Over the course of training, AAV-Cre mice demonstrated impaired learning, as they required significantly longer to find the escape hole compared with their AAV-ΔCre littermates on trials 8 to 12 ($P < 0.043$ for trials 8 to 12) (Fig. 5*A*). During the probe trial on the test day following completion of the 12

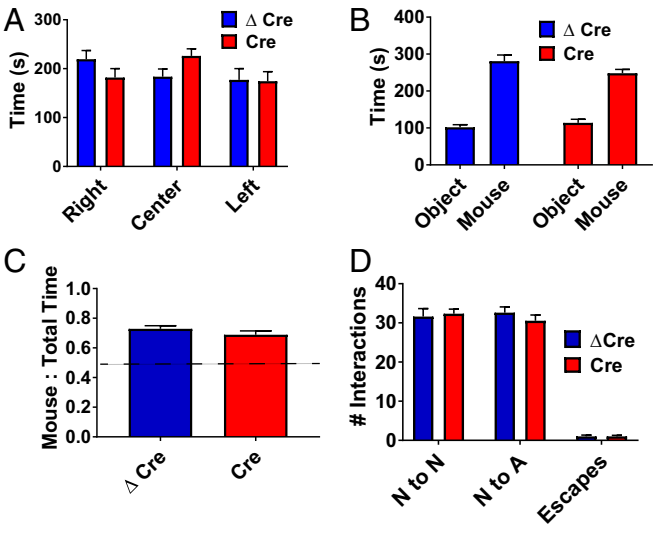

Fig. 4. *Scn1a* deletion in the hippocampus does not cause social interaction deficits. AAV-ΔCre or AAV-Cre–injected *Scn1a* floxed mice were habituated for 10 min in an empty 3-chambered box, removed, and reintroduced to the box following placement of two pencil cups (one empty, one containing a stranger mouse) in opposite chambers. The test mouse was then allowed to freely explore the chambers for 10 min. (*A*) Habituation period for 3-chamber test of social interaction for AAV-ΔCre (blue) and AAV-Cre (red) injected mice. (*B*) Total time (s) spent with either the object (O) or mouse (M). (*C*) Ratio of time spent with mouse to total interaction time with both objects. Unpaired two-tailed Student's *t* test: *Left*, AAV-ΔCre: 0.73 ± 0.021, $n = 16$; *Right*, AAV-Cre: 0.69 ± 0.026, $n = 15$; $P = 0.24$. (*D*) Number of nose-to-nose (N to N), nose-to-anogenital (N to A), and escape behaviors. Data are represented as mean ± SEM.

training trials, AAV-Cre mice spent less time near the escape hole (AAV-ΔCre median: 14.3, $n = 15$; AAV-Cre median 3.05, $n = 16$; $P < 0.0001$) (Fig. 5 *B–D*), took longer to approach the escape hole (AAV-ΔCre median: 4.57, $n = 15$; AAV-Cre median: 54.9, $n = 16$; $P = 0.0055$) (Fig. 5*E*), and exhibited fewer nose pokes into the escape hole (AAV-ΔCre median: 16, $n = 15$; AAV-Cre median: 3.5, $n = 16$; $P = <0.0001$) (Fig. 5*F*). Thus, deletion of *Scn1a* in the hippocampus recapitulated one of the spatial learning deficits seen in global mouse models of Dravet Syndrome.

Spatial learning is often tested in the context of a fearful situation, because fear enhances learning and memory. We measured fear-related spatial learning with the context-dependent fear-conditioning test (31), in which mice associate spatial context with a fear-inducing mild foot shock. Global *Scn1a*$^{+/-}$ mice have a major deficit in this test of fear-related spatial learning. Surprisingly, neither the AAV-Cre nor AAV-ΔCre mice demonstrated defects during context-dependent fear-conditioning. All mice displayed robust freezing behavior after being placed back into a fearful spatial context 30 min, 24 h, and 7 d after a training session in which a mild foot shock was administered in an easily recognizable spatial context (Fig. 6). Therefore, learning and memory deficits in AAV-Cre are specific to spatial learning and memory and can be overcome under more intense fear-induced learning conditions in which the salience of the spatial cues is increased.

Discussion

Global Disease Phenotypes from Local Gene Deletion. Neurogenetic diseases are caused by mutations that are expressed throughout the brain and nervous system. There are few prior examples of diseases in which local genetic changes are found to induce neurologic syndromes that can impact the activity of the entire brain. Previous studies of Dravet Syndrome fit this pattern, in that gene deletion in the entire mouse brain or in subsets of inhibitory neurons throughout the mouse brain cause specific, global disease phenotypes (15, 17, 19–21). Here we take this analysis of Dravet Syndrome pathophysiology to a deeper level by showing that local reduction of $Na_V1.1$ channels in the hippocampus is sufficient to induce brain-wide phenotypes including generalized epilepsy and impaired spatial learning and memory. These global phenotypes may evolve as a consequence of changes in cerebral cortex functionality induced by impaired control of hippocampal excitability. Therefore, these diverse brain-wide phenotypes of Dravet Syndrome may be generated by local changes in neuronal excitability that induce broad effects on electrical activity and cognitive function in the brain.

Inhibitory Neurons in Dravet Syndrome. Like the mutations that cause Dravet Syndrome, our AAV-Cre–mediated gene deletion does not discriminate between excitatory and inhibitory neurons. However, previous work supports the conclusion that effects of mutation of $Na_V1.1$ on inhibitory neurons are primary (10). Heterozygous deletion of $Na_V1.1$ consistently causes reduced excitability of GABAergic inhibitory interneurons in C57BL/6 mice that have the most severe Dravet Syndrome phenotypes (7, 12, 18, 20, 22, 32). Deletion only in inhibitory interneurons causes Dravet Syndrome phenotypes (12, 15, 17, 19). Deletion in excitatory neurons does not induce Dravet Syndrome, and it actually ameliorates some disease phenotypes (22). However, in mice with mixed genetic

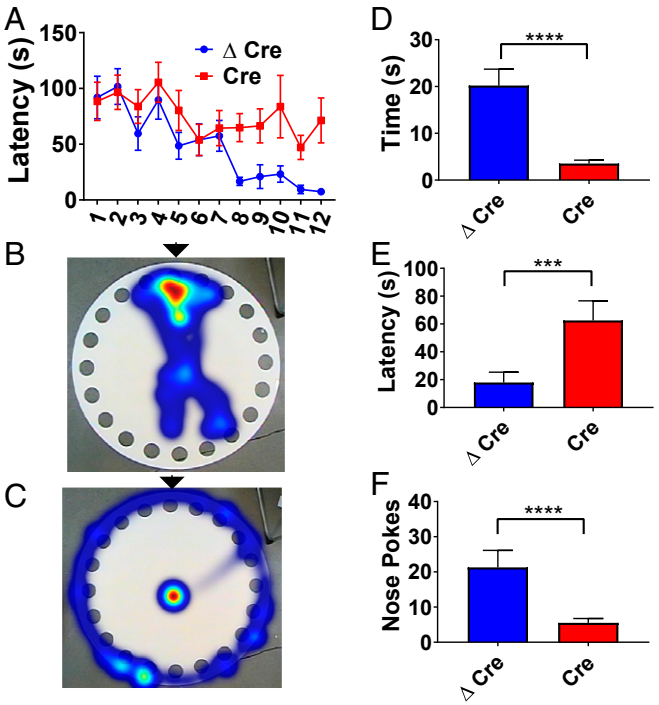

Fig. 5. *Scn1a* deletion in the hippocampus leads to defects in spatial memory. AAV-ΔCre or AAV-Cre–injected *Scn1a* floxed mice were placed on a raised circular platform containing 20 holes. One hole contained a removable escape box. Mice were trained on a series of training trials to find the escape box; when the mouse entered the escape box, the training trial was ended. On the test day, the escape box was removed. (*A*) Latency to escape box during 12 total training trials over 4 d ($P < 0.042$ for trials 8 to 12). (*B*) Heat map of the location of an AAV-ΔCre–injected mouse during the test day trial. Location of escape box during trial days is marked with a black arrow. (*C*) Heat map of the location of an AAV-Cre–injected mouse during the test day trial. Location of escape box during trial days is marked with a black arrow. (*D*) Time spent near correct hole during the test day (Mann–Whitney *U* test; AAV-ΔCre median: 14.3, $n = 15$; AAV-Cre median 3.05, $n = 16$; $P < 0.0001$). (*E*) Latency to target hole during the test day. Mann–Whitney *U* test; AAV-ΔCre median 4.57, $n = 15$; AAV-Cre median 54.9, $n = 16$; $P = 0.0055$. (*F*) Number of times a mouse pokes its nose into the correct hole. Mann–Whitney *U* test; AAV-ΔCre median: 16, $n = 15$; AAV-Cre median: 3.5, $n = 16$; $P = < 0.0001$. ***$P < 0.001$; ****$P < 0.0001$.

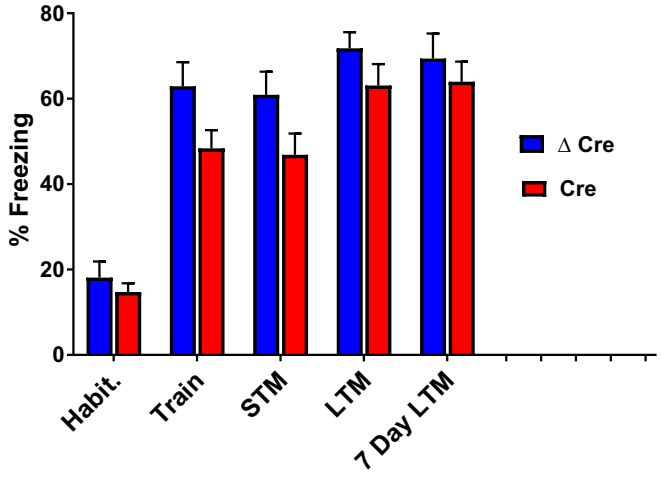

Fig. 6. *Scn1a* deletion in the hippocampus does not cause impairment in context-dependent fear-conditioning. Freezing behavior was recorded in AAV-ΔCre or AAV-Cre–injected *Scn1a* floxed mice during a series of 2-min trials before and at designated time points after a mild foot shock. Mice were habituated for 2 min in a box containing a wire floor grid, after which they received a foot shock. Freezing behavior was calculated during the 2 min habituation (pre-foot shock), training (immediately after foot shock), 30-min short-term memory (STM), 24-h long-term memory (LTM), and 7-d long-term memory trials. Blue = AAV-ΔCre, n = 15; red = AAV-Cre, n = 16. Data are represented as mean ± SEM.

backgrounds and milder Dravet Syndrome phenotypes, increased excitability of excitatory neurons is also observed later in neuronal development, and one study showed that observed deficits in parvalbumin-positive fast-spiking interneurons in the barrel cortex disappeared by P35 (33, 34). These secondary effects of gene deletion may contribute to early development of seizure frequency and intensity in Dravet Syndrome and later amelioration of those phenotypes in adulthood in mice with heterozygous genetic background having a mild Dravet Syndrome phenotype (33). Nevertheless, it is likely that the global disease phenotypes we have observed here are caused by gene deletion in the inhibitory interneurons in the hippocampus. Consistent with this, we observed a selective reduction in GABAergic, but not glutamatergic, signaling to the DGCs when $Na_V1.1$ channels are reduced in the hippocampus. Therefore, we think it is likely that local deletion in inhibitory neurons is responsible for the strong epileptic and cognitive effects we have observed in our mouse model in C57BL/6 mice.

Our studies further support the importance of the hippocampus in seizure initiation and propagation and in spatial learning and memory. Repetitive stimulation of the hippocampus can kindle sustained epilepsy (35). Surgical resection of the hippocampus impairs spatial learning and memory (28). Manipulation of the excitability of the dentate gyrus results in epilepsy in previously healthy mice (36, 37). Hippocampal interneurons have the largest loss of sodium current in Dravet Syndrome mice (7–9, 12, 38). Together with these precedents, our results highlight the hippocampus as a key focus of Dravet Syndrome pathophysiology.

Although our results highlight the importance of the hippocampus for epilepsy and cognitive deficit in Dravet Syndrome, other brain regions also are likely to play a key role in these deficits and other comorbidities. Excitability of interneurons in the cerebral cortex is impaired in Dravet Syndrome mice (18, 38), and this deficit is likely to contribute to epilepsy, cognitive deficit, and autistic-like behaviors in Dravet Syndrome. Impaired electrical excitability of interneurons in the thalamus is likely to be involved in epilepsy and sleep disorder (17). Similarly, impaired excitability of cerebellar Purkinje neurons is likely to be important in the characteristic ataxia of Dravet Syndrome (14). Thus, the comorbidities of Dravet Syndrome are likely to be generated in multiple regions of the brain, but the hippocampus evidently plays a key role in two of the most serious aspects of the disease: epilepsy and cognitive deficit.

Therapeutic Approaches to Dravet Syndrome. As a genetic disease caused by loss-of-function mutations, the ideal long-term therapeutic approach to Dravet Syndrome is to reexpress the affected gene in appropriate brain regions or to use CRISPR/Cas9 methods to repair the gene defect in affected brain regions. While whole-brain reexpression or gene repair might eventually be attainable, and recent papers have indeed demonstrated that broad infection with AAV is possible (39, 40), the risk of widespread off-target effects and the desire for treatment specificity could limit this approach. Our results showing that two of the major deficits in Dravet Syndrome, epilepsy and cognitive deficit, can be generated by gene mutation specifically in the hippocampus open the possibility for future application of gene reexpression or gene repair technologies in the hippocampus using surgical procedures developed for intractable temporal lobe epilepsy. Thus, this study has important implications for understanding the molecular and cellular basis of Dravet Syndrome and for formulating new therapeutic strategies that selectively target the key brain regions contributing to its phenotypes.

Methods

All experiments were carried out in C57BL/6J mouse genetic background. Our methods for mouse husbandry, thermal induction of seizures, and behavioral experiments follow our previously published protocols (11, 12) and are described in detail in *SI Appendix, Methods*. Experiments were performed according to guidelines established in the National Institutes of Health Guide for Care and Use of Laboratory Mice and were approved by the University of Washington Institutional Animal Care and Use Committee.

Viral Production and Infection. Cre- and ΔCre-expressing pAAV1-CBA GFP DNA plasmids were kindly provided by Dr. Larry Zweifel, Department of Psychiatry & Behavioral Sciences and Pharmacology, University of Washington. Briefly, recombination-deficient AAV vectors were grown with AAV1 coat serotype in human embryonic kidney (HEK293T cells). The virus was then purified with sucrose and CsCl gradient centrifugation steps and finally resuspended in 1× HBSS at a functional titer of 1×10^6 (41). Before injection, viral aliquots were stored at −80 °C.

P21 *Scn1a* floxed littermates were randomly assigned to AAV-Cre or AAV-ΔCre groups. Injections were performed at P21, which is the day that they are old enough to be weaned. This eliminated the need to reintroduce the pups to their dam, which can often result in overgrooming and damage to the surgical site. Mice were given an s.c. injection of Ketoprofen (5 mg/kg, Sigma–Aldrich, K2012) 30 to 60 min before the surgery to control for postoperative pain, a procedure that was repeated up to every 24 h for 48 h. The mice were anesthetized with inhaled isoflurane (Piramal Enterprises LTD, NDC 66794–017-25) and placed in a stereotaxic device (Kopf Instruments, Model 962). The hair was shaved above the skull, and bupivacaine (1 mg/kg, AuroMedics Pharma LLC, 167–10) and lidocaine (1 mg/kg, Fresenius Kabi USA, 491257) were injected underneath the skin as a local anesthetic. The skin was cut over the midline, and using a coordinate system (Paxinos and Franklin), holes were drilled in the appropriate locations (dorsal medial hippocampus: −1.9 anterior/posterior [AP], ±1.5 medial/lateral [ML], −1.8 dorsal/ventral [DV]; ventral lateral hippocampus: −3.3 AP, ±2.52 ML, −4, −3, −2 DV). Either AAV-Cre or AAV-ΔCre was injected at a rate of 125 nL/min, and the needle was allowed to sit for 3 min before being withdrawn to prevent backflow. Note that virus injected at these coordinates does not cover the entire hippocampus.

Electrophysiology. Slices harvested from P42 mice injected with virus at P21 were placed in a submersion chamber on an upright microscope and viewed with an Olympus 40× (0.9 N.A.; BX51WI) water-immersion objective with differential interference contrast and infrared optics and were perfused with oxygenated artificial cerebrospinal fluid (aCSF) (2 mL/min). DGCs were distinguished by their location, appearance, and physiological properties. Positive viral expression was assessed by GFP expression. Recordings were only made if positive GFP expression in the dentate gyrus was confirmed. Whole-cell recordings were made using patch pipettes constructed from thick-walled borosilicate glass capillaries and filled with internal solutions optimized for current- or voltage-clamp recordings of sIPSCs or sEPSCs, as described below. Filled patch pipettes had resistances ranging between 3 and 5 MΩ. The internal solution for all current-clamp experiments was as follows (in mM): 132.3 K-gluconate, 7.7 KCl, 4 NaCl, 0.5 $CaCl_2$, 10 Hepes, 5

NEUROSCIENCE

ethylene glycol-bis(β-aminoethyl ether)-*N*,*N*,*N*′,*N*′-tetraacetic acid (EGTA) free acid, 4 ATP Mg^{2+} salt, 0.5 GTP Na^{+} salt, pH buffered to 7.2 to 7.3 with KOH. The internal solution for measuring sIPSCs ($V_h = -60$ mV; ECl = 0 mV) in voltage clamp was as follows (in mM): 130 CsCl, 4 NaCl, 0.5 $CaCl_2$, 10 Hepes, 5 EGTA, 4 ATP Mg^{2+} salt, 0.5 GTP Na^{+} salt, 5 QX-314, pH buffered to 7.2 to 7.3 with CsOH. sIPSCs were measured in the presence of ionotropic glutamate receptor antagonists, CNQX (20 μM) and APV (50 μM). The internal solution for measuring sEPSCs (Vh = –60 mV; ECl = –60 mV) in voltage clamp was as follows (in mM): 145 Cs-Gluconate, 2 MgCl2, 10 Hepes, 0.5 EGTA, 2 ATP-Tris, 0.2 GTP Na^{+} salt, pH buffered to 7.2 to 7.3 with CsOH. Recordings were obtained through a multiclamp 700A amplifier (Molecular Devices) by pCLAMP 8.0 software (Molecular Devices). Drugs were dissolved in aCSF and bath-applied for a minimum of 7 min before analysis. Data from electrophysiology experiments were analyzed using Clampfit 9.0 (Molecular Devices) software. Access resistance was continuously monitored for each cell. Cells were discarded if access resistance changed by >15%. Only one cell was recorded from each brain slice if slices were exposed to pharmacological agents.

EEG Surgeries and Recordings. Surgeries to implant EEG electrodes were performed at P35, 2 wk after the mice had undergone viral injection surgery. This allowed the mice time to recover after the initial surgeries. Both male and female mice were used, and no difference was noticed between the two groups. Mice were given an s.c. injection of Ketoprofen (5 mg/kg, Sigma–Aldrich, K2012) 30 to 60 min before the surgery to control for postoperative pain, a procedure that was repeated up to every 24 h for 2 d. The mice were anesthetized with inhaled isoflurane (Piramal Enterprises LTD, NDC 66794–017-25) and placed in a stereotaxic device (Kopf Instruments, Model 962). The hair was shaved above the skull, and Bupivacaine (1 mg/kg, AuroMedics Pharma LLC, 167–10) and Lidocaine (1 mg/kg, Fresenius Kabi USA, 491257) were injected underneath the skin as a local anesthetic. The skin was cut over the midline, and four silver electrodes were anchored into the skull. Two recording electrodes were placed bilaterally in the cortex, and a third reference electrode was placed into the cerebellum (Fig. 3*C*). A grounding electrode was placed near the left anterolateral edge of the frontal bone. Mice were allowed to recover from the surgery for 1 wk, and EEG recordings were acquired at P42 in conscious mice using a 3-Channel EEG tethered mouse system (Pinnacle Technology Inc, 8200-SE3 Mouse System) during the thermal induction protocol. To correlate seizure activity to EEG activity, mice were simultaneously videotaped for review (WinAVI Video Capture; ZJMedia Digital Technology).

Statistics. All data are expressed as the mean ± SEM or median where noted. For curve comparison, the log-rank (Mantel–Cox) test was used to determine difference between the two conditions as indicated in the figure legends. If data met the assumptions of normally distributed data as determined by Shapiro–Wilk normality test and F test for equal variances, unpaired *t* tests were used for post hoc analysis. For data that failed the assumptions necessary for parametric statistical techniques, we used Mann–Whitney *U* tests where appropriate. For all cases, statistical tests were two-tailed, and the threshold of significance was set at $P < 0.05$. For figures, $*P < 0.05$, $**P < 0.01$, $***P < 0.001$, $****P < 0.0001$.

ACKNOWLEDGMENTS. We thank Dr. Larry Zweifel (Departments of Psychiatry and Behavioral Sciences and Pharmacology, University of Washington) for providing the viral plasmids and Timothy Lantin (University of Washington) for help preparing tissue. The research reported in this publication was supported by the National Institutes of Health project number R01 NS025704 (to W.A.C.), the Alcohol and Drug Abuse Institute, University of Washington, Small Grant Award number ADAI-1016-12 (to J.S.K.), and the National Science Foundation Graduate Research Fellowship Program (to R.E.S.).

1. C. Dravet, Dravet syndrome history. *Dev. Med. Child Neurol.* **53** (suppl. 2), 1–6 (2011).
2. C. Dravet, The core Dravet syndrome phenotype. *Epilepsia* **52** (suppl. 2), 3–9 (2011).
3. L. Claes *et al*., De novo mutations in the sodium-channel gene SCN1A cause severe myoclonic epilepsy of infancy. *Am. J. Hum. Genet.* **68**, 1327–1332 (2001).
4. L. Claes *et al*., De novo SCN1A mutations are a major cause of severe myoclonic epilepsy of infancy. *Hum. Mutat.* **21**, 615–621 (2003).
5. C. Marini *et al*., SCN1A duplications and deletions detected in Dravet syndrome: Implications for molecular diagnosis. *Epilepsia* **50**, 1670–1678 (2009).
6. C. Marini *et al*., The genetics of Dravet syndrome. *Epilepsia* **52** (suppl. 2), 24–29 (2011).
7. F. H. Yu *et al*., Reduced sodium current in GABAergic interneurons in a mouse model of severe myoclonic epilepsy in infancy. *Nat. Neurosci.* **9**, 1142–1149 (2006).
8. I. Ogiwara *et al*., $Na_v1.1$ localizes to axons of parvalbumin-positive inhibitory interneurons: A circuit basis for epileptic seizures in mice carrying an *Scn1a* gene mutation. *J. Neurosci.* **27**, 5903–5914 (2007).
9. W. A. Catterall, F. Kalume, J. C. Oakley, $Na_V1.1$ channels and epilepsy. *J. Physiol.* **588**, 1849–1859 (2010).
10. W. A. Catterall, Dravet syndrome: A sodium channel interneuronopathy. *Curr Opin Physiol* **2**, 42–50 (2018).
11. J. C. Oakley, F. Kalume, F. H. Yu, T. Scheuer, W. A. Catterall, Temperature- and age-dependent seizures in a mouse model of severe myoclonic epilepsy in infancy. *Proc. Natl. Acad. Sci. U.S.A.* **106**, 3994–3999 (2009).
12. S. Han *et al*., Autistic-like behaviour in *Scn1a*$^{+/-}$ mice and rescue by enhanced GABA-mediated neurotransmission. *Nature* **489**, 385–390 (2012).
13. S. Han *et al*., $Na_{(V)}1.1$ channels are critical for intercellular communication in the suprachiasmatic nucleus and for normal circadian rhythms. *Proc. Natl. Acad. Sci. U.S.A.* **109**, E368–E377 (2012).
14. F. Kalume, F. H. Yu, R. E. Westenbroek, T. Scheuer, W. A. Catterall, Reduced sodium current in Purkinje neurons from Nav1.1 mutant mice: Implications for ataxia in severe myoclonic epilepsy in infancy. *J. Neurosci.* **27**, 11065–11074 (2007).
15. F. Kalume *et al*., Sudden unexpected death in a mouse model of Dravet syndrome. *J. Clin. Invest.* **123**, 1798–1808 (2013).
16. S. Ito *et al*., Mouse with Nav1.1 haploinsufficiency, a model for Dravet syndrome, exhibits lowered sociability and learning impairment. *Neurobiol. Dis.* **49**, 29–40 (2013).
17. F. Kalume *et al*., Sleep impairment and reduced interneuron excitability in a mouse model of Dravet syndrome. *Neurobiol. Dis.* **77**, 141–154 (2015).
18. C. Tai, Y. Abe, R. E. Westenbroek, T. Scheuer, W. A. Catterall, Impaired excitability of somatostatin- and parvalbumin-expressing cortical interneurons in a mouse model of Dravet syndrome. *Proc. Natl. Acad. Sci. U.S.A.* **111**, E3139–E3148 (2014).
19. C. S. Cheah *et al*., Specific deletion of $Na_V1.1$ sodium channels in inhibitory interneurons causes seizures and premature death in a mouse model of Dravet syndrome. *Proc. Natl. Acad. Sci. U.S.A.* **109**, 14646–14651 (2012).
20. M. Rubinstein *et al*., Dissecting the phenotypes of Dravet syndrome by gene deletion. *Brain* **138**, 2219–2233 (2015).
21. T. Tatsukawa, I. Ogiwara, E. Mazaki, A. Shimohata, K. Yamakawa, Impairments in social novelty recognition and spatial memory in mice with conditional deletion of *Scn1a* in parvalbumin-expressing cells. *Neurobiol. Dis.* **112**, 24–34 (2018).
22. I. Ogiwara *et al*., Nav1.1 haploinsufficiency in excitatory neurons ameliorates seizure-associated sudden death in a mouse model of Dravet syndrome. *Hum. Mol. Genet.* **22**, 4784–4804 (2013).
23. C. S. Cheah *et al*., Correlations in timing of sodium channel expression, epilepsy, and sudden death in Dravet syndrome. *Channels (Austin)* **7**, 468–472 (2013).
24. J. S. Kaplan, N. Stella, W. A. Catterall, R. E. Westenbroek, Cannabidiol attenuates seizures and social deficits in a mouse model of Dravet syndrome. *Proc. Natl. Acad. Sci. U.S.A.* **114**, 11229–11234 (2017).
25. R. Racine, V. Okujava, S. Chipashvili, Modification of seizure activity by electrical stimulation. 3. Mechanisms. *Electroencephalogr. Clin. Neurophysiol.* **32**, 295–299 (1972).
26. B. D. Winters, S. E. Forwood, R. A. Cowell, L. M. Saksida, T. J. Bussey, Double dissociation between the effects of peri-postrhinal cortex and hippocampal lesions on tests of object recognition and spatial memory: Heterogeneity of function within the temporal lobe. *J. Neurosci.* **24**, 5901–5908 (2004).
27. S. D. Vann, M. M. Albasser, Hippocampus and neocortex: Recognition and spatial memory. *Curr. Opin. Neurobiol.* **21**, 440–445 (2011).
28. R. G. Morris, P. Garrud, J. N. Rawlins, J. O'Keefe, Place navigation impaired in rats with hippocampal lesions. *Nature* **297**, 681–683 (1982).
29. H. Eichenbaum, C. Stewart, R. G. Morris, Hippocampal representation in place learning. *J. Neurosci.* **10**, 3531–3542 (1990).
30. C. A. Barnes, Memory deficits associated with senescence: A neurophysiological and behavioral study in the rat. *J. Comp. Physiol. Psychol.* **93**, 74–104 (1979).
31. J. N. Crawley, Behavioral phenotyping of transgenic and knockout mice: Experimental design and evaluation of general health, sensory functions, motor abilities, and specific behavioral tests. *Brain Res.* **835**, 18–26 (1999).
32. M. Rubinstein *et al*., Genetic background modulates impaired excitability of inhibitory neurons in a mouse model of Dravet syndrome. *Neurobiol. Dis.* **73**, 106–117 (2015).
33. A. M. Mistry *et al*., Strain- and age-dependent hippocampal neuron sodium currents correlate with epilepsy severity in Dravet syndrome mice. *Neurobiol. Dis.* **65**, 1–11 (2014).
34. M. Favero, N. P. Sotuyo, E. Lopez, J. A. Kearney, E. M. Goldberg, A transient developmental window of fast-spiking interneuron dysfunction in a mouse model of Dravet syndrome. *J. Neurosci.* **38**, 7912–7927 (2018).
35. E. W. Lothman, J. L. Stringer, E. H. Bertram, The dentate gyrus as a control point for seizures in the hippocampus and beyond. *Epilepsy Res. Suppl.* **7**, 301–313 (1992).
36. E. Krook-Magnuson, G. G. Szabo, C. Armstrong, M. Oijala, I. Soltesz, Cerebellar directed optogenetic intervention inhibits spontaneous hippocampal seizures in a mouse model of temporal lobe epilepsy. *eNeuro* **1**, e.2014 (2014).
37. E. Krook-Magnuson *et al*., In vivo evaluation of the dentate gate theory in epilepsy. *J. Physiol.* **593**, 2379–2388 (2015).
38. U. B. Hedrich *et al*., Impaired action potential initiation in GABAergic interneurons causes hyperexcitable networks in an epileptic mouse model carrying a human Na(V) 1.1 mutation. *J. Neurosci.* **34**, 14874–14889 (2014).
39. B. E. Deverman *et al*., Cre-dependent selection yields AAV variants for widespread gene transfer to the adult brain. *Nat. Biotechnol.* **34**, 204–209 (2016).
40. G. Massaro *et al*., Fetal gene therapy for neurodegenerative disease of infants. *Nat. Med.* **24**, 1317–1323 (2018).
41. B. B. Gore, M. E. Soden, L. S. Zweifel, Manipulating gene expression in projection-specific neuronal populations using combinatorial viral approaches. *Curr. Protoc. Neurosci.* **65**, 4.35.1–4.35.20 (2013).